

## RESEARCH ARTICLE

# Identification of new candidate molecules against SARS-CoV-2 through docking studies

Punar Aliyeva<sup>1</sup>  | Beyza Yilmaz<sup>2</sup>  | Doruk Alp Uzunarslan<sup>3</sup>  | Vildan Enisoglu Atalay<sup>4\*</sup> <sup>1</sup> Uskudar University, Graduate School of Science, Department of Molecular Biology, 34662, Istanbul, Türkiye  
ROR ID: [02dzjmc73](https://orcid.org/02dzjmc73)<sup>2</sup> Uskudar University, Graduate School of Science, Department of Biotechnology, 34662, Istanbul, Türkiye  
ROR ID: [02dzjmc73](https://orcid.org/02dzjmc73)<sup>3</sup> Uskudar American Academy, 34674, Istanbul, Türkiye<sup>4</sup> Informatics Institute, Computational Science and Engineering, Istanbul Technical University, 34469, Istanbul, Türkiye  
ROR ID: [059636586](https://orcid.org/059636586)\* Corresponding author: E-mail: [enisogluatalayv@itu.edu.tr](mailto:enisogluatalayv@itu.edu.tr) ; Ph.: +90 (212) 444 1 488; Fax: +09 (212) 285 29 10

**Citation:** Aliyeva, P., Yilmaz, B., Uzunarslan, D.A., & Enisoglu-Atalay, V. (2025) Identification of new candidate molecules against SARS-CoV-2 through docking studies. *The European chemistry and biotechnology journal*, 4, 14-23. <https://doi.org/10.62063/ecb-40>

**License:** This article is licensed under a Creative Commons Attribution-NonCommercial 4.0 International License (CC BY-NC 4.0).

**Peer review:** Double Blind Refereeing.

**Received:** 23.10.2024

**Accepted:** 16.05.2025

**Online first:** 27.05.2025



## Abstract

The recent outbreak of a new coronavirus disease known as COVID-19, caused by Severe Acute Respiratory Syndrome Coronavirus 2 (SARS-CoV-2), is a highly contagious and pathogenic viral infection that has spread worldwide. Coronaviruses are known to cause disease in humans, other mammals, and birds. Although specific therapeutics and vaccines require efforts in this direction, reaching the world's population with mutations of the virus can be a difficult target. The major proteases of coronavirus play a critical role during the spread of the disease and therefore still represent an important target for drug discovery. As of now, there is still no official treatment for infected patients. In this study, bioinformatics-based molecular docking studies were performed to identify potent inhibitors of novel candidate molecules against the spike protein S of SARS-CoV-2. The affinities of ligand molecules thought to be effective in the treatment of SARS-CoV-2 disease were investigated. For this purpose, 1,615 different FDA-approved drug ligand molecules were retrieved from ZINC15 database. Crystallographic structure of spike protein S of SARS-CoV-2 was retrieved from Protein Data Bank (PDB). Initial virtual screening was performed using *qvina-w*, an accelerated version of AutoDock Vina optimized for rapid docking, to evaluate binding affinities of all 1,615 compounds against the spike protein. The top 10 ligands with the most favorable binding affinities were selected for further analysis. These ligands were docked to the target protein with Autodock Vina. The complexes were first solvated and then run through Molecular Dynamics (MD) simulations, utilizing NAMD. The binding energies were computed through these interactions, which are used to compare the affinities of the ligands to the target protein. Ultimately, 10 different ligands

capable of inhibiting the spike protein of SARS-CoV-2 were selected and compared based on their affinities.

**Keywords:** Coronavirus, in silico, Molecular Docking, Drug Development

## Introduction

The acute respiratory infection that we know as the novel coronavirus SARS-CoV-2 was first identified in Wuhan China in the year 2019 (Petersen et al. 2020). This infection is highly contagious and can be transmitted via droplet and contact. Coronavirus (CoV) belongs to the family Coronaviridae, suborder Cornidovirineae, and order Nidovirales. According to the phylogenetic analysis, the Coronaviridae family can be classified into 4 genera, namely alpha, beta, delta, and gamma (Payne 2017). Human and animal cells are both susceptible to infection by the single stranded RNA virus known as the coronavirus, which has a positive virulence. Human coronaviruses are among the rapidly evolving viruses, because of their high recombination rate and nucleotide element dominance (Fehr and Perlman 2015). Several recent reports, both genome wide and at the receptor level provided unique insights on many characteristics of the SARS-CoV-2 virus. One of these characteristics include the ability of different variants of SARS-CoV-2 to bind to Angiotensin-Converting Enzyme 2 (ACE2) cell receptors (Letko et al 2020). It is the binding of the spike protein (S) to the ACE2 receptor that allows SARS-CoV-2 to enter cells, as it facilitates the initiation of viral replication (Shang, J et al, 2020; Wang et al 2020).

SARS-CoV-2 is a virus with a long, single-stranded RNA genome, about 30,000 bases in length. This genome is one of the largest among all known RNA viruses, which boosts the virulence of the virus through reduced dependence on host cells for replication. The virus itself is small, measuring between 50-200 nanometers, and is covered with spike-like proteins that help invade human cells. SARS-CoV-2 is responsible for causing Severe Acute Respiratory Syndrome (SARS), which affects the respiratory system and can lead to serious complications (Payne, 2017). The symptoms of infection can vary widely among individuals. While some patients experience mild, cold-like symptoms, others suffer from severe respiratory distress or long-term complications, often referred to as “long COVID.” This variability in how the virus impacts individuals highlights the complexity of SARS-CoV-2 and its interactions with the human body.

Coronaviruses display spherical structure and include the following four main types of structural proteins; membrane (M), envelope (E), nucleocapsid (N) and spike (S) protein (Fehr and Perlman, 2015). Membrane protein lies within the range of 25 to 30 kDa and has three transmembrane N-terminal domains, a glycosylated ectodomain and a C terminal domain (Armstrong et al., 1984). The M protein is diamimic protein that fuses other outer structural proteins, foreboding the virus to bud out (Neuman et al., 2011). Envelope protein has an approximate mass of about 8 to 12 kDa (Schoeman and Fielding, 2019). The E protein consists of the N terminal ectodomain and C terminal endodomain (Nietto-Torres et al., 2014). The E protein increases the pathogenicity of the virus by acting on its ion channel as transmembrane proteins during the process of budding and the release of the virus (Li et al., 2014). The N protein has N terminal and C terminal domains.

The N protein is rich in phosphate esters and phosphates in general (Stohlman and Lai, 1979). Because of the strong binding of N proteins to viral RNA, the N protein associates with the viral RNA genome and encapsulates it (Kuo and Masters 2013). The N protein assists in the packaging of the

viral RNA genome into the replicase-transcriptase complex (RTC) and afterwards the virus genome into the viral virus (Hurst et al. 2013).

Spike protein has a vital role in SARS-CoV-2 virus transmission (Shang et al., 2020). Attachment initiates with the trimetric spike protein's S1 subunit's interaction with ACE2 receptors in the heart, kidneys, and lungs (Hamming et al., 2004). S1 and S2 separation in the SARS-CoV-2 spike protein takes place owing to the presence of the proprotein convertase (PPC) section (Walls et al., 2020). The S protein is subsequently cleaved at the host cell membrane by the transmembrane serine protease 2 (TMPRSS2) which results in the release of S1 subunit while triggering the S2 subunit to become rearranged to a post-fusion conformation that assists in the merging of the viral and host cell membranes (Bestle et al., 2020). The peptide domain that is able to modulate this action comes from the S2 subunit and is activated via receptor recognition, allowing it to breach the host cell membrane (Xiu et al., 2020). Delta and Omicron variants have highlighted the importance of targeting conserved viral elements, as these variants exhibit increased transmissibility and resistance to neutralizing antibodies (Shuai et al., 2022).

The primary objective of molecular docking is to characterize and predict molecular recognition, through structural (identifying alternate binding modes) and energy-wise compatibility. Computer-based methods shorten the drug design process, providing low cost and speed drug development environments, while, contributing to the analysis of the interaction between ligands and the target protein structure by calculating the binding affinity (Kitchen et al., 2004). *In silico* studies, molecular docking in particular, have accelerated the identification of potential inhibitors targeting SARS-CoV-2 proteins. Examples include the identification of drugs that could bind to the spike protein receptor-binding domain through docking studies (Garg et al., 2021; Santos-Martins et al., 2021). Computational techniques have been employed for fast, affordable, and efficient compound screening, paving the way for drug discovery.

In this study, molecular docking simulations are used to identify novel molecules capable of inhibiting the spike protein found in SARS-CoV-2. By evaluating binding affinities and physicochemical properties of ligand candidates, this work aims to contribute to the ongoing efforts of developing therapeutic strategies against SARS-CoV-2 and its evolving variants. FDA-approved molecules identified as inhibitors of the relevant target structure through the ZINC15 database were included in the study as ligand molecules.

## Materials and methods

To obtain the crystal structures of the proteins important for SARS-CoV-2, the ACE2-linked structure with PDB ID 6M0J (Figure 1) at 2.45 Å resolution was selected from the Protein Data Bank (<https://www.rcsb.org/>) database (Lan et al., 2020). In order to perform multiple docking operations in a concise manner, it was essential to define a specific region of interest on the protein surface where ligand binding is most likely to occur. The gridbox center coordinates for 6M0J were determined as  $x=-31.454$ ,  $y=29.553$ ,  $z=21.871$  and a gridbox box with a size of  $40 \times 40 \times 40 \text{ Å}^3$  was determined. In this study, 1,615 different FDA-approved molecules were retrieved from the ZINC15 database (<https://zinc15.docking.org>). These molecules were then docked to the target protein. Through Autodock Vina, the binding affinities of the candidate molecules were scored and compared. The obtained physicochemical parameters of the ligand candidate molecules for effective treatment of SARS-CoV-2 disease were taken into consideration. All the docking studies were implemented using Autodock Vina (Eberhardt et al., 2021). After docking studies were performed, the interaction maps

of the ligands with the target protein structures were investigated in detail. The topmost 10 ligands were selected ranked by their binding affinities. These ligands were simulated for 2 nanoseconds using NAMD. Subsequently, the overall energy change was observed between the ligands and the target protein.

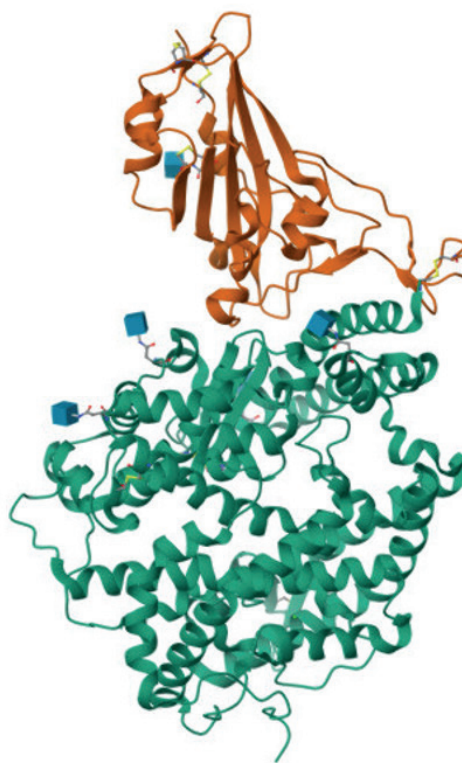


**Figure 1.** Crystal structure of SARS-CoV-2 spike receptor-binding domain bound with ACE2.

## Results and discussion

Table 1 shows molecular weights and lipophilicities of candidate molecules that were docked against S spike protein of SARS-CoV-2. These physicochemical parameters, including molecular weight (Mw) and lipophilicity (logP), play a crucial role in determining the pharmacokinetic behavior of the ligands, such as absorption, distribution, and membrane permeability.

**Table 1. Calculated Properties of the Investigated Ligands (Top 100 Ranked by Binding As**

ZINC ID	Mw	logP	BE	ZINC000253387843	924.091	0.712	-8.7
ZINC000052955754	581.673	1.991	-10.1	ZINC000252286876	926.107	0.778	-8.7
ZINC000252286878	926.107	0.778	-9.7	ZINC000253630390	875.106	5.601	-8.6
ZINC000203757351	765.893	3.637	-9.2	ZINC000150338819	889.017	8.607	-8.4
ZINC000242548690	780.949	2.218	-9.1	ZINC000068202099	485.506	5.822	-8.2
ZINC000003927200	366.501	4.306	-8.8	ZINC000001530886	514.629	7.264	-8.2
ZINC000003978005	583.689	2.081	-8.8	ZINC000100378061	570.646	3.48	-8.2
ZINC000027990463	693.732	8.382	-8.8	ZINC000000968264	287.406	4.698	-8.2

ZINC000003784182	412.529	6.681	-8.2	ZINC000072318121	506.605	4.937	-7.6
ZINC000252286877	926.107	0.778	-8.2	ZINC000150338708	761.85	3.413	-7.6
ZINC000040430143	434.471	2.347	-8.1	ZINC000001612996	586.689	4.091	-7.5
ZINC000169621215	847.019	4.616	-8.1	ZINC000034089131	433.592	4.972	-7.5
ZINC000150588351	882.035	8.116	-8	ZINC000169621220	665.733	0.12	-7.5
ZINC000100013130	570.649	5.907	-8	ZINC000003882036	394.439	0.62	-7.5
ZINC000000538658	448.95	5.683	-8	ZINC000084758235	546.937	4.51	-7.5
ZINC000003985982	414.498	3.125	-8	ZINC000003860453	332.311	3.666	-7.5
ZINC000095617678	810.466	5.719	-8	ZINC000100073786	562.706	4.24	-7.5
ZINC000169289767	872.894	6.67	-8	ZINC000004074875	610.671	6.319	-7.5
ZINC000169621228	877.045	5.648	-8	ZINC000000897240	381.907	4.298	-7.5
ZINC000003932831	528.537	6.576	-8	ZINC000035902489	450.345	5.038	-7.5
ZINC000028232746	723.65	2.462	-7.9	ZINC000035328014	440.507	4.217	-7.5
ZINC000203686879	883.019	7.732	-7.9	ZINC000003816514	500.483	5.73	-7.5
ZINC000004175630	461.556	6.269	-7.9	ZINC000003920266	497.5	1.02	-7.5
ZINC000164528615	838.878	3.857	-7.9	ZINC000016052277	444.44	0.702	-7.5
ZINC000003918087	543.525	0.001	-7.8	ZINC000100017856	366.844	5.505	-7.5
ZINC000204073689	492.591	5.63	-7.8	ZINC000261527196	690.86	2.269	-7.5
ZINC000011681563	578.601	6.787	-7.8	ZINC000003993846	506.709	4.051	-7.5
ZINC000036701290	532.57	4.456	-7.8	ZINC000100370145	562.706	4.24	-7.5
ZINC000003927822	492.689	4.256	-7.8	ZINC000100013500	517.776	5.251	-7.4
ZINC000006716957	529.526	6.356	-7.8	ZINC000000643143	531.44	4.206	-7.4
ZINC000169621200	785.891	6.158	-7.8	ZINC000003931840	517.776	5.251	-7.4
ZINC000253632968	749.956	5.254	-7.8	ZINC000066166864	482.628	4.773	-7.4
ZINC000003872566	501.667	5.511	-7.7	ZINC000011617039	437.529	3.139	-7.4
ZINC000012503187	498.586	6.507	-7.7	ZINC000095551509	766.918	4.142	-7.4
ZINC000019632618	493.615	4.59	-7.7	ZINC000103105084	324.38	2.519	-7.4
ZINC000003831128	429.604	5.407	-7.7	ZINC000013831130	444.423	1.486	-7.4
ZINC000000538550	412.946	3.809	-7.7	ZINC000085537026	748.996	1.901	-7.4
ZINC000164760756	749.956	5.254	-7.7	ZINC000111460375	562.706	4.24	-7.4
ZINC000053683151	654.606	3.193	-7.7	ZINC000005844792	405.441	2.364	-7.4
ZINC000150338755	868.457	8.66	-7.7	ZINC000000004724	252.273	2.642	-7.4
ZINC000252286875	926.107	0.778	-7.7	ZINC000001539579	348.486	6.104	-7.4
ZINC000169621219	729.908	3.438	-7.7	ZINC000218037687	868.948	4.957	-7.4
ZINC000004213474	454.966	3.889	-7.6	ZINC000169621231	958.24	6.197	-7.4
ZINC000118912450	332.484	4.401	-7.6	ZINC000043207238	444.524	2.968	-7.4
ZINC000011616852	723.65	2.462	-7.6	ZINC000030691420	408.922	2.021	-7.4
ZINC000004213946	405.441	2.364	-7.6	ZINC000053683271	690.86	2.269	-7.4
ZINC000004214700	426.492	3.081	-7.6	ZINC000150601177	894.127	7.687	-7.4
ZINC000064033452	452.413	4.747	-7.6	ZINC000306122005	540.708	1.43	-7.4
ZINC000008220909	665.733	0.12	-7.6	ZINC000009574770	812.018	4.929	-7.3
ZINC000014261579	540.697	4.704	-7.6				
ZINC000169289388	914.187	6.181	-7.6				
ZINC000003917708	527.526	1.029	-7.6				



As demonstrated in Table 1, it is evident that the binding affinities of the candidate ligands to the S spike protein of SARS-CoV-2 vary significantly.  $-7.0$  kcal/mol is acknowledged as a threshold for high protein-ligand binding affinity. As clearly shown on Table 1, multiple candidate ligands surpass this threshold with a relatively high margin. This underlines the fact that alternative options for highly affinitive ligands exist ubiquitously among FDA approved ligands.

Moreover, the 10 most suitable ligands compared based on Binding Affinities (kcal/mol) are put into molecular dynamics simulation for further analysis. The protein–ligand complex was subjected to a 2 nanosecond molecular dynamics simulation using Nanoscale Molecular Dynamics (NAMD) (Philips *et al.*, 2020). After the simulation was complete, visualization and trajectory analyses were performed using Visual Molecular Dynamics (VMD) (Humphrey, 1996). The system was solvated in a TIP3P water box, neutralized with counterions, and simulated under periodic boundary conditions using the CHARMM36 force field. Insights from these simulations will help identify ligands with both strong and stable interactions, potentially guiding future *in vitro* validation and drug repurposing efforts against SARS-CoV-2.

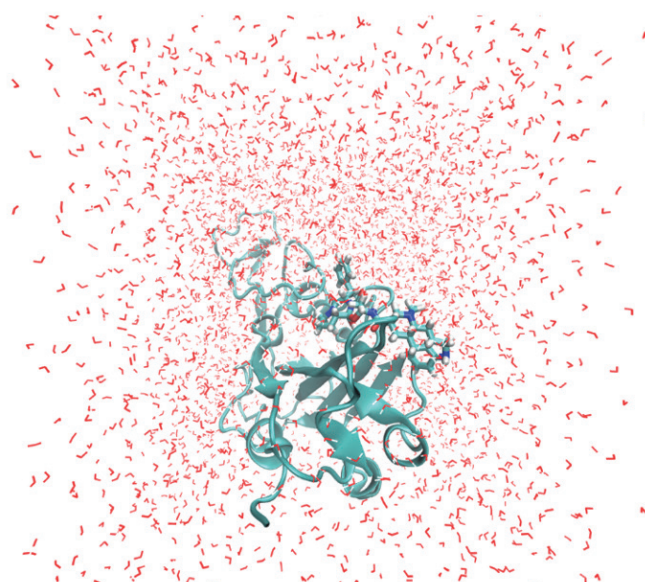


| **Figure 2.** ZINC000052955754 Docked to spike protein S of SARS-CoV-2.

Figure 2 shows the complex formed by ZINC000052955754 and spike protein S of SARS-CoV-2. Taking Table 1 into consideration, this ligand shows high binding affinity towards the spike protein of SARS-CoV-2. After this initial docking analysis, the complex was subjected to molecular dynamics simulation to evaluate the stability and behavior of the ligand within the binding pocket over time. Non-bonded interactions between the ligand and the protein were calculated through NAMD to provide a better viewpoint on the inhibition feature of the ligand. Calculated frame-by-frame, the mean of interaction energy was calculated as  $-62.811$  kcal/mol. The negative value of the interaction energy suggests that the binding process is thermodynamically favorable and likely spontaneous under physiological conditions. This energy profile reinforces the notion that ZINC000052955754 forms a stable and energetically favorable complex with the spike protein.

## Conclusions

This study identified potential candidate molecules for inhibiting the SARS-CoV-2 spike protein by molecular docking studies. Among the 1,615 compounds screened, the top ten candidates were further investigated through molecular docking and molecular dynamics simulations. The frequent and significant interactions between these ligands and the amino acids suggest their potential as inhibitors against SARS-CoV-2 spike protein. Furthermore, ligand with the ZINC ID of ZINC000052955754 demonstrated a strong and spontaneous interaction with the spike protein, supported by a mean interaction energy of -62.811 kcal/mol. These findings emphasize the potential of repurposing existing drugs as effective inhibitors of SARS-CoV-2. *In silico* methodologies applied in this study provide a cost-effective and efficient pathway for drug discovery. These results align with the understanding that structural compatibility between the ligand and active site is crucial for achieving high binding affinity. Moreover, the results reinforce the importance of structural complementarity and physicochemical optimization in achieving high-affinity protein–ligand interactions. Future work should focus on experimental validation through *in vitro* and *in vivo* assays to confirm the therapeutic potential of these candidates. Expanding the compound library and enhancing computational accuracy will further strengthen the applicability of such approaches in addressing current and emerging viral threats.

## Acknowledgements

None.

## Funding

None.

## Conflict of interest

The authors declare no conflict of interest.

## Data availability statement

Data can be obtained from the corresponding author upon a reasonable request.

## Ethics committee approval

Ethics committee approval is not required for this study.

## Authors' contribution statement

The authors acknowledge their contributions to this paper as follows: **Study conception and design:** P.A., B.Y., D.A.U., V.E.A.; **Data collection:** P.A., B.Y., D.A.U., V.E.A.; **Analysis and interpretation of results:** P.A., B.Y., D.A.U., V.E.A.; **Manuscript draft preparation:** P.A., B.Y., D.A.U., V.E.A. All authors reviewed the results and approved the final version of the manuscript.

## ORCIDs and emails of the authors

Punar Aliyeva | ORCID 0000-0002-2868-0736 | [pnar\\_aliyeva@mail.ru](mailto:pnar_aliyeva@mail.ru)

Beyza Yilmaz | ORCID 0009-0007-5768-5070 | [beyza.yilmaz@st.uskudar.edu.tr](mailto:beyza.yilmaz@st.uskudar.edu.tr)

Doruk Alp Uzunarslan | ORCID 0009-0001-4223-7984 | [duzunarslan27@my.uaa.k12.tr](mailto:duzunarslan27@my.uaa.k12.tr)

Vildan Enisoglu Atalay | ORCID 0000-0002-9830-9158 | [enisogluatalayv@itu.edu.tr](mailto:enisogluatalayv@itu.edu.tr)

## References

- Armstrong, J., Niemann, H., Smeekens, S., Rottier, P., & Warren, G. (1984). Sequence and topology of a model intracellular membrane protein, E1 glycoprotein, from a coronavirus. *Nature*, 308(5961), 751–752. <https://doi.org/10.1038/308751a0>
- Beniac, D. R., Andonov, A., Grudeski, E., & Booth, T. F. (2006). Architecture of the SARS coronavirus prefusion spike. *Nature Structural & Molecular Biology*, 13(8), 751–752. <https://doi.org/10.1038/nsmb1123>
- Bestle, D., Heindl, M. R., Limburg, H., Pilgram, O., Moulton, H., Stein, D. A., Harges, K., Eickmann, M., Dolnik, O., Rohde, C., Klenk, H. D., Garten, W., Steinmetzer, T., & Böttcher-Friebertshäuser, E. (2020). TMPRSS2 and furin are both essential for proteolytic activation of SARS-CoV-2 in human airway cells. *Life Science Alliance*, 3(9), e202000786. <https://doi.org/10.26508/lsa.202000786>
- Bhattacharya, S., Banerjee, A., & Ray, S. (2021). Development of new vaccine target against SARS-CoV2 using envelope (E) protein: An evolutionary, molecular modeling and docking based study. *International Journal of Biological Macromolecules*, 172, 74–81. <https://doi.org/10.1016/j.ijbiomac.2020.12.192>
- Bosch, B. J., Van der Zee, R., De Haan, C. A., & Rottier, P. J. (2003). The coronavirus spike protein is a class I virus fusion protein: Structural and functional characterization of the fusion core complex. *Journal of Virology*, 77(16), 8801–8811. <https://doi.org/10.1128/JVI.77.16.8801-8811.2003>
- Daina, A., Michielin, O., & Zoete, V. (2017). SwissADME: A free web tool to evaluate pharmacokinetics, drug-likeness and medicinal chemistry friendliness of small molecules. *Scientific Reports*, 7, 42717. <https://doi.org/10.1038/srep42717>
- Eberhardt, J., Santos-Martins, D., Tillack, A. F., & Forli, S. (2021). AutoDock Vina 1.2.0: New docking methods, expanded force field, and python bindings. *Journal of Chemical Information and Modeling*, 61(8), 3891–3898. <https://doi.org/10.1021/acs.jcim.1c00203>
- Fehr, A. R., & Perlman, S. (2015). Coronaviruses: An overview of their replication and pathogenesis. In H. J. Maier, E. Bickerton, & P. Britton (Eds.), *Coronaviruses: Methods and Protocols* (pp. 1–23). Humana Press. [https://doi.org/10.1007/978-1-4939-2438-7\\_1](https://doi.org/10.1007/978-1-4939-2438-7_1)
- Frenoy, P., Perduca, V., Cano-Sancho, G., Antignac, J. P., Severi, G., & Mancini, F. R. (2022). Application of two statistical approaches (Bayesian Kernel Machine Regression and Principal Component Regression) to assess breast cancer risk in association to exposure to mixtures of brominated flame retardants and per- and polyfluorinated alkylated substances in the E3N cohort. *Environmental Health*, 21(1), 27. <https://doi.org/10.1186/s12940-022-00817-0>
- Garg, M., Maralakunte, M., Garg, S., Dhooria, S., Sehgal, I., Bhalla, A. S., Vijayvergiya, R., Grover, S., Bhatia, V., Jagia, P., Bhalla, A., Suri, V., Goyal, M., Agarwal, R., Puri, G. D., & Sandhu, M. S. (2021). The conundrum of ‘Long-COVID-19’: A narrative review. *International Journal of General Medicine*, 14, 2491–2506. <https://doi.org/10.2147/IJGM.S316708>
- Hamming, I., Timens, W., Bulthuis, M. L. C., Lely, A. T., Navis, G. V., & van Goor, H. (2004). Tissue distribution of ACE2 protein, the functional receptor for SARS coronavirus. A first step in understanding SARS pathogenesis. *The Journal of Pathology*, 203(2), 631–637. <https://doi.org/10.1002/path.1570>



- Humphrey, W., Dalke, A., & Schulten, K. (1996). VMD - Visual Molecular Dynamics. *Journal of Molecular Graphics*, 14(1), 33–38. [https://doi.org/10.1016/0263-7855\(96\)00018-5](https://doi.org/10.1016/0263-7855(96)00018-5)
- Hurst, K. R., Koetzner, C. A., & Masters, P. S. (2013). Characterization of a critical interaction between the coronavirus nucleocapsid protein and nonstructural protein 3 of the viral replicase-transcriptase complex. *Journal of Virology*, 87(16), 9159–9172. <https://doi.org/10.1128/JVI.01075-13>
- Kamimura, A., Umemoto, H., Kawamoto, T., & Honda, T. (2021). Development of water solubility of 2-phenylsulfanylhydroquinone dimer dye. *ACS Omega*, 6(13), 9254–9262. <https://doi.org/10.1021/acsomega.1c00507>
- Kitchen, D. B., Decornez, H., Furr, J. R., & Bajorath, J. (2004). Docking and scoring in virtual screening for drug discovery: Methods and applications. *Nature Reviews Drug Discovery*, 3(11), 935–949. <https://doi.org/10.1038/nrd1549>
- Kumawat, P., Agarwal, L. K., & Sharma, K. (2024). An overview of SARS-CoV-2 potential targets, inhibitors, and computational insights to enrich the promising treatment strategies. *Current Microbiology*, 81, 169. <https://doi.org/10.1007/s00284-024-03615-1>
- Kuo, L., & Masters, P. S. (2013). Functional analysis of the murine coronavirus genomic RNA packaging signal. *Journal of Virology*, 87(9), 5182–5192. <https://doi.org/10.1128/JVI.03478-12>
- Lan, J., Ge, J., Yu, J., Shan, S., Zhou, H., Fan, S., Zhang, Q., Shi, X., Wang, Q., Zhang, L., & Wang, X. (2020). Structure of the SARS-CoV-2 spike receptor-binding domain bound to the ACE2 receptor. *Nature*, 581(7807), 215–220. <https://doi.org/10.1038/s41586-020-2180-5>
- Letko, M., Marzi, A., & Munster, V. (2020). Functional assessment of cell entry and receptor usage for SARS-CoV-2 and other lineage B betacoronaviruses. *Nature Microbiology*, 5(4), 562–569. <https://doi.org/10.1038/s41564-020-0688-y>
- Li, Y., Surya, W., Claudine, S., & Torres, J. (2014). Structure of a conserved Golgi complex-targeting signal in coronavirus envelope proteins. *Journal of Biological Chemistry*, 289(18), 12535–12549. <https://doi.org/10.1074/jbc.M113.528487>
- Molinspiration. (2015). Calculation of molecular properties and bioactivity score. <http://www.molinspiration.com/cgi-bin/properties>
- Neuman, B. W., Kiss, G., Kunding, A. H., Bhella, D., Baksh, M. F., Connelly, S., Droese, B., Klaus, J. P., Makino, S., & Buchmeier, M. J. (2011). A structural analysis of M protein in coronavirus assembly and morphology. *Journal of Structural Biology*, 174(1), 11–22. <https://doi.org/10.1016/j.jsb.2010.11.021>
- Nieto-Torres, J. L., DeDiego, M. L., Verdiá-Báguena, C., Jimenez-Guardeño, J. M., Regla-Nava, J. A., Fernandez-Delgado, R., Castano-Rodriguez, C., Alcaraz, A., Torres, J., Aguilera, V. M., & Enjuanes, L. (2014). Severe acute respiratory syndrome coronavirus envelope protein ion channel activity promotes virus fitness and pathogenesis. *PLoS Pathogens*, 10(5), e1004077. <https://doi.org/10.1371/journal.ppat.1004077>
- Payne, S. (2017). Family Coronaviridae. In *Viruses* (pp. 149–158). Academic Press. <https://doi.org/10.1016/B978-0-12-803109-4.00017-9>
- Petersen, E., Koopmans, M., Go, U., Hamer, D. H., Petrosillo, N., Castelli, F., Storgaard, M., Al Khalili, S., & Simonsen, L. (2020). Comparing SARS-CoV-2 with SARS-CoV and influenza

- pandemics. *The Lancet Infectious Diseases*, 20(9), e238–e244. [https://doi.org/10.1016/S1473-3099\(20\)30484-9](https://doi.org/10.1016/S1473-3099(20)30484-9)
- Phillips, J. C., Hardy, D. J., Maia, J. D. C., Stone, J. E., Ribeiro, J. V., Bernardi, R. C., Buch, R., Fiorin, G., Hénin, J., Jiang, W., McGreevy, R., Melo, M. C. R., Radak, B. K., Skeel, R. D., Singharoy, A., Wang, Y., Roux, B., Aksimentiev, A., Luthey-Schulten, Z., Kalé, L. V., Schulten, K., Chipot, C., & Tajkhorshid, E. (2020). Scalable molecular dynamics on CPU and GPU architectures with NAMD. *The Journal of Chemical Physics*, 153(4), 044130. <https://doi.org/10.1063/5.0014475>
- Rarey, M., Wefing, S., & Lengauer, T. (1996). Placement of medium-sized molecular fragments into active sites of proteins. *Journal of Computer-Aided Molecular Design*, 10(1), 41–54. <https://doi.org/10.1007/BF00124466>
- Rogers, D. M., Agarwal, R., Vermaas, J. V., Durrant, J. D., Welborn, V. V., Kireev, D., & Luthey-Schulten, Z. (2023). SARS-CoV2 billion-compound docking. *Scientific Data*, 10, 173. <https://doi.org/10.1038/s41597-023-02148-0>
- Schoeman, D., & Fielding, B. C. (2019). Coronavirus envelope protein: Current knowledge. *Virology Journal*, 16, 69. <https://doi.org/10.1186/s12985-019-1182-0>
- Sharma, V., Rai, H., Gautam, D. N. S., Prajapati, P. K., & Sharma, R. (2022). Emerging evidence on Omicron (B.1.1.529) SARS-CoV-2 variant. *Journal of Medical Virology*, 94(5), 1876–1885. <https://doi.org/10.1002/jmv.27526>
- Stohman, S. A., & Lai, M. M. (1979). Phosphoproteins of murine hepatitis viruses. *Journal of Virology*, 32(2), 672–675. <https://doi.org/10.1128/jvi.32.2.672-675.1979>
- Walls, A. C., Park, Y. J., Tortorici, M. A., Wall, A., McGuire, A. T., & Veersler, D. (2020). Structure, function, and antigenicity of the SARS-CoV-2 spike glycoprotein. *Cell*, 181(2), 281–292.e6. <https://doi.org/10.1016/j.cell.2020.02.058>
- Wang, Q., Qiu, Y., Li, J. Y., Zhou, Z. J., Liao, C. H., & Ge, X. Y. (2020). A unique protease cleavage site predicted in the spike protein of the novel pneumonia coronavirus (2019-nCoV) potentially related to viral transmissibility. *Virologica Sinica*, 35, 337–339. <https://doi.org/10.1007/s12250-020-00206-5>
- Wang, Y., Grunewald, M., & Perlman, S. (2020). Coronaviruses: An updated overview of their replication and pathogenesis. In H. J. Maier, E. Bickerton, & P. Britton (Eds.), *Coronaviruses: Methods and Protocols* (pp. 1–29). Humana. [https://doi.org/10.1007/978-1-0716-0327-7\\_1](https://doi.org/10.1007/978-1-0716-0327-7_1)
- Xia, S., Liu, M., Wang, C., Xu, W., Lan, Q., Feng, S., Qi, F., Bao, L., Du, L., Liu, S., Qin, C., Sun, F., Shi, Z., Zhu, Y., Jiang, S., & Lu, L. (2020). Inhibition of SARS-CoV-2 (previously 2019-nCoV) infection by a highly potent pan-coronavirus fusion inhibitor targeting its spike protein that harbors a high capacity to mediate membrane fusion. *Cell Research*, 30(4), 343–355. <https://doi.org/10.1038/s41422-020-0305-x>
- Xiu, S., Dick, A., Ju, H., Mirzaie, S., Abdi, F., Cocklin, S., Zhan, P., & Liu, X. (2020). Inhibitors of SARS-CoV-2 entry: Current and future opportunities. *Journal of Medicinal Chemistry*, 63(21), 12256–12274. <https://doi.org/10.1021/acs.jmedchem.0c00502>